Achieving large-scale, high-resolution, full shell replicated x-ray optics: budgeting for sources of spatial resolution errors

J. Kolodziejczak[a], J. Gaskin*[a], W. Baumgartner[a], S. Bongiorno[a], P. Champey[a], D. Gurgew[b], B. Ramsey[a], S. P. Singam[c], C. Speegle[a], N. Thomas[a]
[a]Marshall Space Flight Center, [b]Universities Space Research Association, Science and Technology Institute; [c]Oak Ridge Associated Universities, National Space Science and Technology Center, 320 Sparkman Dr., Huntsville, AL USA 35805;

ABSTRACT

Technology for a large-area, high-angular resolution mirror module for a future Great Observatory x-ray mission is progressing along different paths. To date, none of these are fully developed. Work at the Marshall Space Flight Center (MSFC) seeks to leverage the benefits of full shell optics while exploring the limits of using shell replication technology for optics production. Here, we provide an updated accounting of spatial-resolution-constraining error terms to give context to recent improvements in MSFC replicated optics, as well as guidance and justification for current and future directions of research. Content includes strawman error allocations for an optical system that is parametrically *Lynx*-like, where the replicated-optics technology stands relative to these allocations, and methodology for mapping development plans to efficiently identify the limiting factors and approaches to overcoming these.

Keywords: high-resolution x-ray optics, error budget

1. INTRODUCTION

Future space-based x-ray missions desire large effective area in given energy bands, and fine angular-resolution. The surface area per unit effective area is simply the inverse of graze angle, typically 50-100. This leads to cost models dominated by minimizing errors in optical surfaces on large scales and makes spatial resolution the primary cost discriminator. An error budget for angular resolution is an explicit breakdown of the sources of errors in optical surfaces for a given technology. Every term in the error budget has a story, not just in terms of contribution to the overall spatial resolution, but also in terms of effort required to achieve and demonstrate technology readiness, and potential contribution to cost. The objective of this paper is to outline an approach for establishing an error budget for one such technology, full-shell replicated optics, in the context of x-ray optics technology development at MSFC.

Typically, science observations of a given duration are limited by either photon counts, background counts, or neighboring source counts. It is often the case that the largest possible effective area and the smallest possible spatial resolution is desired. Effective area and angular resolution are tabulated for a list of realized and conceptual large missions in Table 1.

Table 1. On-going and conceptual large x-ray missions' effective areas and half-power diameter (HPD) angular resolutions are listed.

Name	Effective Area (cm^2 at 1.5 keV)	Angular Resolution (arcsec, HPD)
Chandra [1]	~700	0.5
XMM [2]	~4650	16
NewAthena [3]	~10,000	5-10
Lynx [4]	~20,000	0.5
Gen-X [5,6]	~500,000 – 1,000,000	0.1

The cost of achieving high resolution, for example, limited the achievable effective area of *Chandra* and the resolution of *XMM*. Realizing future missions requires reducing the costs of high-angular resolution through focused, and early, technical advancements.

*jessica.gaskin@nasa.gov; phone 256-962-7818

2. MSFC OBJECTIVES

2.1 Replicated Optics at MSFC

The replicated full-shell x-ray optics work at MSFC has a long history (examples are listed in Table 2). While these missions and ground-based efforts have required a range of angular-resolutions and effective areas, recent research has focused on technology advancements for improving the angular resolution. Much of the progress developing high-angular-resolution mirrors has been leveraged from smaller projects with minimal development time and cost.

Table 2. List of past and current replicated optics projects at MSFC.

Name (Application)	Approximate Year(s)	Hi-res required	Reference
AXAF-S - *Constellation-X* (Astrophysics)	1990-2002	No	[7-9]
HERO- HEROES (Astrophysics)	2006-2023	No	[10-12]
SRG ART-XC (Astrophysics)	2012-2016	No	[13-15]
IXPE (Astrophysics)	2017-2020	No	[16,17]
MiXO (Planetary)	2015-2023	No	[18]
MaGIXS (Heliophysics)	2019-2023	Yes	[19,20]
Sandia-NIF-NIST-NIH (Ground-based)	2005-2021	Yes (NIF)	[21-27]
FOXSI (Heliophysics)	2011-2023	Yes	[28-32]
RedSOX (Astrophysics)	2017-2023	No	[33,34]

2.2 Capabilities and Recent Developments

To fabricate replicated x-ray optics, the MSFC team has produced designs, processes, and procedures at varying levels of angular resolution beginning at near arcminute with recent developments to near arcsec [24]. The resolution-sensitive steps in the process include diamond turning, lap-polishing, and CNC polishing of mandrels, replication (which involves plating and separation), and assembly or module-integration of shells. Just as important, measurement capabilities include nanometer-level interferometric measurement of mandrels and shell figure and finish, in-situ instrumentation for sub-micron positioning and monitoring during assembly, and x-ray calibration facilities for shell and mirror-module testing [32,35,36].

Recent angular-resolution improvements have stemmed from progress along several process threads. For a 54 mm diameter x 70 mm long mandrel for NIF, we've developed CNC polishing and metrology data collection procedures to improve figure convergence to 2 nm RMS, leading to < 2" HPD predicted performance for a perfect shell from this more error sensitive small mandrel [24]. 2-3" HPD CNC performance was repeated on 64 and 70 mm diameter by 300 mm long mandrels for the *FOXSI-4* project [31]. Typical prior values were ~8" for 300 mm long mandrel segments after diamond turning and lap polishing operations. Improvements in lap polishing resulting from the *IXPE* project, yielded the best mandrels with ~5" HPD at the completion of lap polishing, as a result of optimized lap design and polishing parameters based on lap polishing simulations.

Replication of small shells at MSFC had been plagued by sensitivity to end effects in both polishing and replication. These were combatted in the NIF project through a design which included relief segments at both ends and at the intersection. The relief segments allowed the polishing bonnet to continue to the end of the optical surfaces so that the entire surface could be made to match the prescription while redirecting impinging rays far from the focus. The segments also provide a buffer zone to prevent end-replication-induced distortions from contributing directly to the performance, while also adding a small amount of stiffness against circularity deformations. In parallel, we have developed plating bath simulations [37] to inform the design of auxiliary components such as gaskets and shields to minimize the variation in thickness and stress in the shell. An important side effect of these improvements was enabling thicker shells to be electroformed without premature separation due to built-up end stresses. The direct benefit to improved axial figure is relatively small, as azimuthally asymmetries in components and separation tend to dominate. The effects of azimuthal asymmetries have been difficult to reproduce in simulations. Nevertheless, our best shell, a 4.5" HPD, 2.3" FWHM, 1 mm thick NIF shell, was the product of these improvements.

Assembly of shells into a module requires positioning and bonding in place with proper alignment and minimal distortion. Angular resolution is relatively insensitive to alignment, so we have placed a tight allocation on this error budget term. Our capabilities have improved to within allocation through improved precision of positioning and in-situ metrology [32,35]. Depending on thickness, even slight contact with a replicated shell can easily distort it beyond 0.5". Assembly methods have improved in the last 5 years from a point where assembly distortions contributed >10" HPD, to our current best case of 0.5". This has come about via improved shell offloading while suspended, beginning with *IXPE*. Limitations in measuring the axial bend ($\Delta\Delta R$) in the shell surface arose in *IXPE* because of imprecision in the bearing that supported a rotating sensor array. More recently, an air bearing used for *FOXSI-4* assembly, enables $\Delta\Delta R$ determination at the 0.5" HPD level. This, combined with careful monitoring and compensation for thermal drifts in the support structure, have resulted in the noted improvement.

We currently do not have in-situ metrology for our CNC machine. The mandrel is removed, and its axial figure is measured with an interferometer at a series of meridians after each polishing pass. The improvements in mandrel performance were due in part to improved repeatability of measurements and registration between the CNC machine and interferometer, resulting from the use of a precision pallet system that enables the mandrel to be transferred between work stations with accurate repeatability. We find that consecutive measurements on untouched mandrel sections lead to repeatability of 0.4" RMS slope errors, and fits of differences in metrology between consecutive passes to the predicted wear pattern have residuals <2 nm RMS. Through simulations that account for sequential reduction in bonnet sizes to optimally access smaller amplitude higher frequency errors, we predict that our current mandrel performance capability is 1.5" HPD, much improved from our best lap polishing, but still limited mainly by metrology.

The current focus of our research is to gain more insight on the tall poles in the error budget. The largest is replication, and we continue to address both electroforming and separation aspects. More frequent simulation and measurement-driven adjustments to plating bath parameters will be implemented to account for bath changes and the growing shell's effects on the electric field. Instrumenting the shell surface with strain sensors prior to release to monitor the characteristics and path of separation will provide insights to further guide development of separation strategies.

Characterization of the axial figure of recent small-diameter high-resolution shells is an important diagnostic that has been hampered by the size limitations of our long-trace profilometer. Since larger diameters are required, we plan to polish larger mandrels to high resolution and use them for future process development. This will permit use of the long-trace profilometer, so we can better characterize the shell distortions, as well as enabling investigation at a more realistic scale. In parallel, to more efficiently measure the shell optical surface using a computer-generated hologram (CGH) system in conjunction with the interferometer, is under development.

Mandrel performance capability limitations result from our manual metrology data collection process. A discrete number of axial profiles are collected, and repeatability in the circumferential registration, as well as interpolation errors between meridian contribute to the convergence limit noted above. An automated data collection system is being implemented to eliminate metrology as a mandrel performance constraint, both by more accurately positioning the mandrel azimuthally and enabling higher circumferential sampling density.

Recent assembly experience with *IXPE* and *FOXSI-4* suggests that our current module designs are susceptible to global shell-distorting forces during the final assembly steps following installation of shells. For *IXPE*, this contributed 10-15" HPD and for *FOXSI-4* it was 5-7" because of bending of the spider structure upon which the shells are bonded. To achieve high resolution, a design and assembly process which precludes these distortions is required. This will be a necessary part of the larger-shell development effort mentioned above.

In testing *FOXSI-4* modules, in-focus HPDs in the range 7-12" were observed at the same orientation with different mounting techniques, suggesting as much as 10" of mounting distortion, resulting from a legacy mounting design which was not intended for high resolution optics. This design aspect must also be considered in the next iteration. Clearly, achieving high-resolution requires an end-to-end process where all significant contributors at every step are accounted for and controlled. This fact is reflected in the error budget presented below.

The *Chandra* mission successfully tested a large-scale high-resolution optic in a 1-g environment. We do not have the number of scientists and engineers involved in simulating and designing off-loading mechanisms for the test environment that were available for a Great Observatory. We know that a horizontal 1-g test of thin high-resolution optics will be more challenging than *Chandra*, so we need to continue to develop x-ray testing techniques and procedures to accurately evaluate performance from test data in order to continue to make progress toward 0.5" resolution. Some of these were applied to *FOXSI-4* testing, but two facts are apparent: 1) in-focus data cannot be accurately interpreted without high-fidelity simulations, and 2) effects of gravity are most easily separated from

inherent distortions through the analysis of out-off focus images at multiple roll angles. To this end, the modules we develop for test would provide the most utility if the mounting approach is both simple to simulate and repeatable in terms of the distortions imparted at the desired roll angles. These ideas will also be applied to our next iteration.

Table 3. Some advantages and limitations of full shell replicated optics.

Advantages	Limitations
• **Fewer pieces than segmented approach.** Fewer pieces mean fewer parts and fewer procedure steps to track, and quality assure. • **Fewer contact points than segmented.** Contact or bonding points are potential sources of distortion. • **Smaller edge to surface ratio than segmented.** Generally, edge effects lead to distortions or require compensation. • **Segment-pair alignment is not required**. Axial alignment is provided by mandrel. • **Less susceptible to distortions due to coating.** Symmetry provides robustness against coating stresses. • **Multiple shells from 1 polished mandrel.** If direct shell polishing is not required, then a multimodule approach would yield module-count scaled polishing-cost savings. • **Compensating distortions.** A constant axial slope error over the full-shell length compensates in the ray error, and the natural response of a shell to a local distortion is dominated by compensating deformations, so performance is degraded less for a given size distortion in a full shell.	• **Tooling must scale with diameter.** A large investment in tooling for large diamond turning machines, polishers, and plating bathes for large-diameter mandrel production. • **Material properties are inferior to mono-crystalline silicon.** Modulus of elasticity, micro-yield sensitivity and yield strength are all smaller, for materials currently considered, leading to more susceptibility to distortions due to handling, gravity, and other applied forces. • **Full shell limits access to optical surface for direct measurements.** Segment surfaces are easier to measure. • **Full shells are less portable and more difficult to handle than segments.** Larger shells require large handling fixtures to prevent damage in transport. • **Some advantages disappear at large diameters**. Susceptibility to distortions due to coating, and compensating distortion advantages dimmish with increasing diameter.

2.3 Assessing the Full Shell Option

Full-shell replicated optics offer numerous advantages over other technologies, but also have challenges, especially with increasing shell diameter. We highlight a sampling of these in Table 3.

The technological landscape for large-scale high-resolution x-ray optics contains several promising candidates. Segmented monocrystalline silicon optics, currently achieving <3” HPD [38] for assemblies and 0.8” for a single pair, has the ability to scale to virtually any size without scaling up on size capacity of fabrication equipment. Unfigured silicon-pore optics are currently limited to *Athena*-level resolution and adaptive concepts have not yet demonstrated high-resolution capability. Technology for full shell replicated optics has shown signs that rapid advancement in performance is possible, with current capability <5” HPD on smaller diameter shells. Until this performance can be demonstrated on larger-scale mirror shells, the technology readiness for larger mirror assemblies remains at a TRL 3-4 (medium-resolution MSFC full-shell replicated optics are much higher TRL). The number of error budget terms for any technology is likely to rise rapidly with improving angular resolution. A prudent strategy is to continue along diverse paths that appear to have potential in the relatively short-term. MSFC full-shell replicated technology is among these.

2.4 Approach to Achieving High Spatial Resolution

Fabricating a surface that conforms to prescription at sub-arcsecond precision can be done with decades-old technology. The current challenges are staying within cost constraints for fabricating ~100 m^2 of surface to this precision, and then maintaining it throughout an entire process involving shell replication, handling, coating, alignment, assembly, test, integration, launch and operation in the space environment. (Understand, improve, assure)

Efficient development efforts focus on three objectives necessary for achieving high-angular resolution. These are understanding requirements, identifying or developing process engineering technology, and identifying, monitoring, and controlling key process parameters. An error budget is a central tool fitting these pieces together.

Each stage in the process needs to enable high resolution. A process step will influence resolution and exercising the step physically or through simulation provides the insight needed to extract process requirements. The requirement is just the relationship between a parameter in the process and its influence on resolution. A complete error budget would include all the process influences on resolution, and the inverse influence functions applied to the budgeted allocations

give a starting point for required constraints on process parameters. Development is the process of give and take, comparing allocation with improving capability to get the roll up to match an anchoring top-level requirement.

Improving capability entails identifying or developing process engineering technology. A high precision manufacturing process starts with and feeds back into the optics module design. It is neither the case that the design drives the manufacturing process, or the process drives the design. Instead, the design is part of the process. Materials, facilities, equipment, instrumentation, procedures, and simulations are all part of process engineering technology. If technology is added to the process, it is added either to enable constraint of a performance-sensitive parameter, reduce cost, or increase assurance of the process step completing successfully.

Enforcing parameter constraints and assuring success rely on ability to identify, monitor, and control key driving process parameters. When a submicron distortion can lead to degradation in angular resolution, embedded verification steps are required to assure success. The error budget identifies the drivers and is a tool for setting requirements on the monitoring and control capabilities. The R&D effort loops back through analysis of monitored parameters and correlation, to further our understanding and define which research paths will further improve capability.

3. AN ERROR BUDGET FOR SPATIAL RESOLUTION

In the absence of a driving flight program with known requirements, the importance of the error budget is not to ensure that requirements are met but to be used as a development tool. The uses of the tool include developing a systematic way to understand and communicate the sources of error, associating development tasks with error terms to better focus efforts within the tasks toward addressing the sources of error, and establishing metrics within development tasks to compare with allocated errors to use in planning and prioritizing future efforts.

Resources to address every error term are not an available luxury. Process metrics measure a specific capability. The insight gained by comparing error allocation with capability provides a mechanism to identify tall poles in the negative margin category. To make progress toward achieving the top-level allocation, tall poles need to be addressed at a higher priority.

The method for developing this error budget is a process which parallels the overall development effort. It is necessary to assign quantities in a phased manor. Initial assignment of allocations is a simple flow-down based on the equipartition of parent errors among children and some experience and knowledge from error budgets of past projects such as *Chandra*. Further refinement is fed by the results of simulations and tests where the relationship between an error term and a performance metric is tested. In an idealized case, the entire end-to-end process would be simulated, in which case the error budget represents a view of the process' ideal and real state. The nuance of knowledge of our true capability is captured in two ways: through the assignment of a "typical" and "best" values, and by assigning an uncertainty to the error terms.

3.1 Errors vs. Requirements and Buy-off.

A closely nested high-resolution x-ray optical assembly will necessarily have as-thin-as-possible optical elements and as a result, is likely to be sensitive to component displacements and distortions at the submicron level. It is therefore essential to understand the likelihood of and sensitivity to distortion-inducing force application at every step in the fabrication, assembly, test, and integration process. Any induced errors that go unnoticed will likely not be caught until a later stage when a measurement or test is performed to "buy-off" a higher-level requirement. Buy-off is meant to indicate that all risks associated with the process steps up to that point have been retired. In the context of high resolution, the risks are such that an error budget term is exceeded in some process step, leading to a failure to meet the higher-level requirement.

The error budget needs to parallel the anticipated workflow to capture the potential error contributions inherent in each process step. The error budget term "driver" needs to be limited to prevent the error-producing distortion or uncertainty. In some cases, the error budget term driver is specified as a design, process, and/or data requirement, and in others it may be assessed as unlikely enough to be exceeded that it does not need an associated requirement.

The assessment of risk while mapping between error terms and requirements is a means of evaluating the need for intermediate verifications, the type of verification, e.g. test, inspection, analysis or combinations, and the type and quality of data required. High-resolution means that a smaller distortion influences the angular performance. Thinner optics means the same amount of force produces a large distortion. As a result, a much more rigorous level of intermediate verification is necessary to ensure success at the buy-off stage. The technology development provides

the foundation for the necessary rigor by producing and then working within the context of an error budget derived from the end-to-end manufacturing process.

For a start, we have developed a spreadsheet format which accommodates the information (columns) listed in Table 4 for each error budget term (row). Revisions to this structure are inevitable as R&D progresses. A large portion of the current R&D process is to accurately populate these columns and find methods to improve the margins to positive values. We chose the typical/best terminology to describe the current state because often data points arise from vastly different approaches or small samples, where statistical uncertainty is difficult to derive or interpret. It may be useful to think of these in terms of technology readiness level (TRL). The process meets the bottom rung of the TRL ladder when minimal positive margin is attained. It is then possible to advance up the ladder by improving the typical margin, then scaling to larger size mirrors and testing in realistic environments as appropriate.

Table 4. Information associated with each error budget term.

Name	Description
Level	Number of parent-child steps below the top level, which is 0. These are error budget levels and not requirements levels.
Item number	Arbitrary sequential number for each item in a level
Subitem number	Sequential number for each subitem within an item. Subitems are not children.
Identifier	Level. Item number. Subitem number
Parent Identifiers	Identifier of error-term parents
Descriptive Name	Descriptive name for the error term
Verification Method	For error terms that are requirements, a verification method is identified, e. g. x-ray test, optical test, analysis and simulation.
Allocation	Estimate of error value required to achieve top-level allocation in arcsec, HPD
Uncertainty	Estimate of uncertainty in error value required to achieve top-level allocation
Sensitivity	Mathematical relationship between the driver and error term
Driver allocation	Estimate of value required to achieve top-level allocation in driver units
Typical	Typical level achieved in development tasks
Best	Best level achieved in development tasks
Typical margin	(Driver allocation - Typical) / (Driver allocation) × 100
Best margin	(Driver allocation - Best) / (Driver allocation) × 100
Driver units	Units of the driving quantity
Notes	Place to tabulate other information

In the description that follows, we will not present these details. Instead, we have simply an A-value for “allocation” and a C-value for “capability”. In most cases, these are in “arcsec, HPD”, and we provide a terse justification for the capability value, which is derived from a best-case scenario. We present the error budget in 3 categories: Post-Assembly, Shells and Assembly, and Generic. The Post-Assembly illustrates aspects of the buy-off stages. The Shells and Assembly is the primary focus of our technology development efforts. Generic items are not unique to full-shell replication, but apply to all flight-capable x-ray optics. Figure 1 shows the top 4 levels of the error budget with color coding for these 3 categories indicated in the caption. The anchor allocation is 0.5 arcsec, HPD at 1.5 keV, based on measured in-flight performance after 1 year. While currently not specified, we assume an energy band and effective area consistent with a *Lynx*-like configuration with large shell count. At this stage in the error budget formulation, we are very specific about items that affect the structure of the error budget and remain flexible regarding the focal length and exact shell count, size and coating. Aside from the roll-up terms, labeled 0.1.0, 1.1.0, and 2.1.0, gray and orange boxes provide mainly context, and their allocations are based on *Chandra*, which is the only comparable mission. The capabilities in the gray and orange boxes are rough estimates.

3.2 Post-assembly: testing and aging

Modeled after the approach of *Chandra*, we anticipate that a ground test of the mirror assembly will be required to buy-off the roll-up of manufacturing process-induced risks to meeting the angular-resolution requirement. Even with *Chandra*’s massive mirrors, it was not possible to directly reproduce 0-g performance in ground test. The addition of ground-to-flight corrections comparable to predicted performance were necessary in the analysis of ground data. Moving to thinner shells will likely make ground-to-flight corrections larger, assuming x-ray testing in a horizontal

beamline. For this error budget, the post-assembly aspects are placeholders, and we assume that capabilities will roughly match what *Chandra* achieved, which is the basis of our allocation.

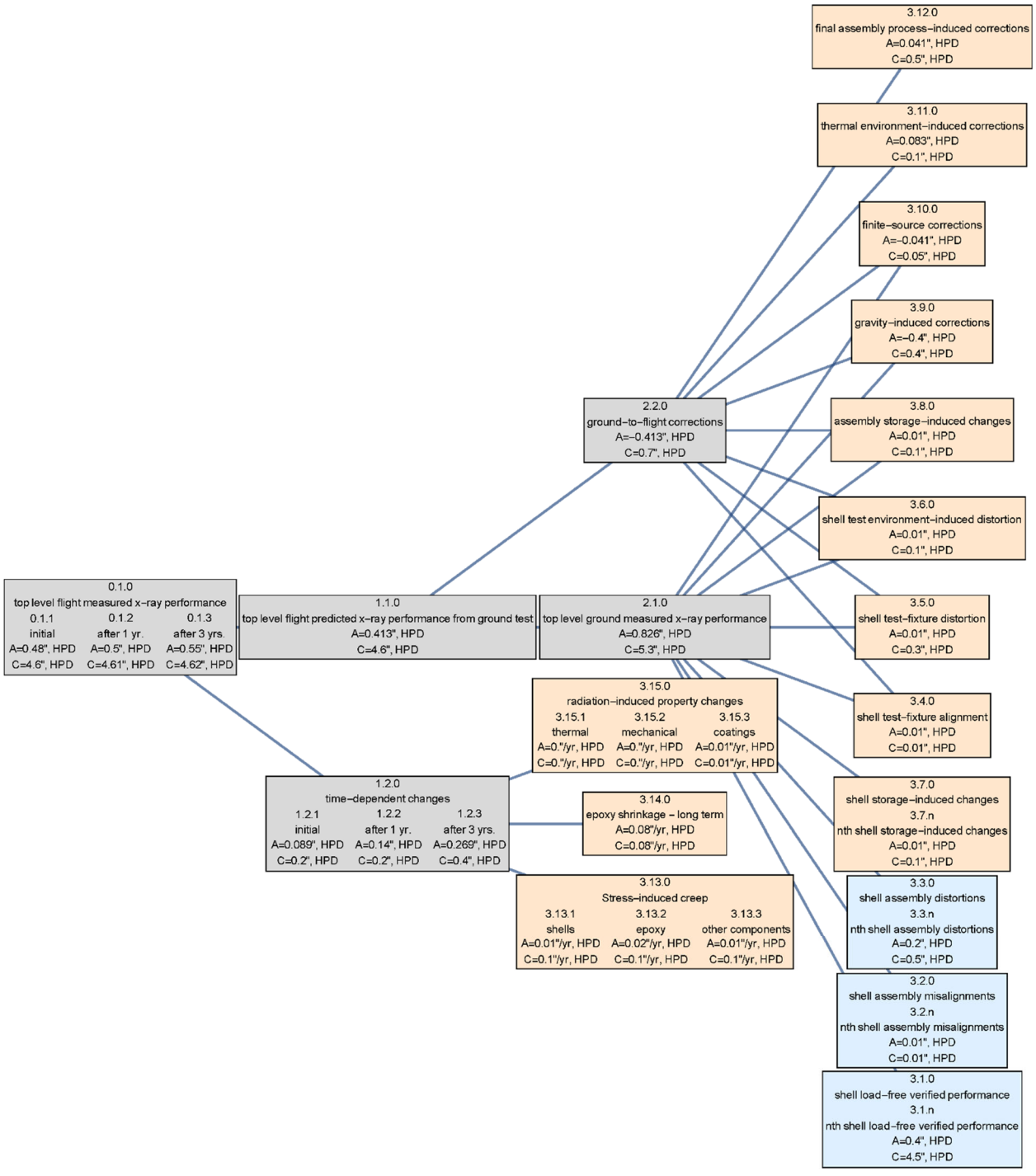

Figure 1. Top 4 levels of an error budget for a high-resolution full shell replicated optical system. The light gray boxes parallel the post-assembly stage of integration where error sources are testing and aging related. The light orange boxes account for Generic items, which we view as relatively independent of the manufacturing technology. The light blue boxes parallel the steps for fabrication and assembly of mirror shells, addressing error sources arising from processes and metrology. The terms labeled 3.1.0, 3.2.0 and 3.3.0 are further detailed in Sec. 3.3.

The flexibility of thinner optical substrates requires more attention to time-dependent effects. For this reason, we include budget terms for long-term degradation. At Level 0, three subitems specify performance 0, 1 and 3 years after the start of operations. We take the one-year allocated value as nominally 0.5 arcsec, HPD, from which all the other allocations ensue. Straight-forward verification from flight data provides these final buy-offs of risks derived from aging mechanisms the uncertainties of the ground-to-flight corrections.

At Level 1, the flight prediction from ground test and aging expectations feed into the Level 0, so the aging term is also broken out into 0-, 1- and 3-year subitems. The allocations for these derive from items included under Generic items and are discussed further in Sec. 3.4. The prediction is needed as a test-plus-analysis verification to justify launch. It is included to maintain the correspondence between the error budget and the anticipated actual process.

The Level 2 children of the flight prediction from ground test are the ground-measured x-ray performance and the ground-to-flight corrections. The allocations for these derive from items included under Generic items and like the aging items are discussed further in Sec. 3.4. In a sense, the net effect of the ground-to-flight corrections is zero, since they add to the ground-measured value, but are subtracted in the corrected prediction. Their purpose in the error budget is to represent the risk of mistakes and account for uncertainties. In a more refined iteration, some fraction of the uncertainty in this term will be included in the flight prediction. We discuss the three manufacturing-related children of the ground-measured x-ray performance in Sec. 3.3.

3.3 Shells and assembly: processes and metrology

The core elements of replicated-shell technology are fabricating the shells and assembling them into nested modules. Aside from ground-to-flight corrections, at Level 3 the three items that determine the ground measured performance are each shell's load-free verified performance, the alignment of each shell with respect to the others, and the distortion that each shell's optical surface undergoes in the assembly process. The allocations for these are in proportion to our perception of the difficulty of each term. The capability values are based on our best-case results [32] mentioned in Sec.2.2.

Figure 2 is a breakout of the shell load-free verified performance. The assembly process is serial and practically irreversible, so confidence in the performance of each shell being added to the assembly is paramount. The term "load-free verified' is explicit here because we do not want to risk degrading a large assembly of shells by installing a defective one. The means of verification will inevitably involve collecting a combination of x-ray test and metrology data and analyzing it, so there are likely to be additional error terms not shown here that are analogous to the ground-to-flight corrections term discussed in Sec. 3.2, with "flight" being analogous to "load-free." To reduce redundancy and complexity, we left these terms out of the error-tree and replaced them with the term "load-free verified". A future iteration will contain these additional terms once the verification process is more clearly defined.

At level 4, the shell performance children are the mandrel predicted performance, replication-induced distortions, shell-polishing convergence limit, coating-induced distortions, and coating inherent surface roughness. The mandrel predicted performance is the value that is expected for the performance of an undistorted load-free shell. The capability value is based on known limits of metrology repeatability and best-case experience with computer-controlled polishing. The allocation and capabilities for the coating-induced affects are rough estimates. These could be viewed as generic, however they are a part of our active R&D. We also plan to develop the capability to direct polish replicated shells in case progress stalls on improvement in replication. An allocation for this is included in the error budget, but the capability is currently ignored in the roll-up.

Replication-induced distortions are a key element of our current R&D efforts and a current tall pole in the error budget with a best margin of -2900%. We attribute most of the difference between best-mandrel predicted performance and best-shell performance to the replication process, and the capability value reflects this. The allocation and capability numbers at Levels below 4 are derived from rough estimates and equipartitioning of errors among children at this time, but through modeling and simulations we are working to refine these numbers and find ways of improving the process capability [37].

Mandrel predicted performance capabilities are well-understood and broken down in a way that allows us to identify where improvements are needed. For example, azimuthally varying errors are worse than cylindrically symmetric errors because we are limited in the number of azimuthal meridians over which we collect interferometric metrology. This leads to interpolation errors between meridians. We are developing a more automated system for mandrel metrology to remedy this deficiency. While there is still a large discrepancy between the capability and allocation, the

path for improving mandrel performance capability is much clearer than for replication. We know adequate polishing technology exists, so our in-house capability is not considered a technology tall pole.

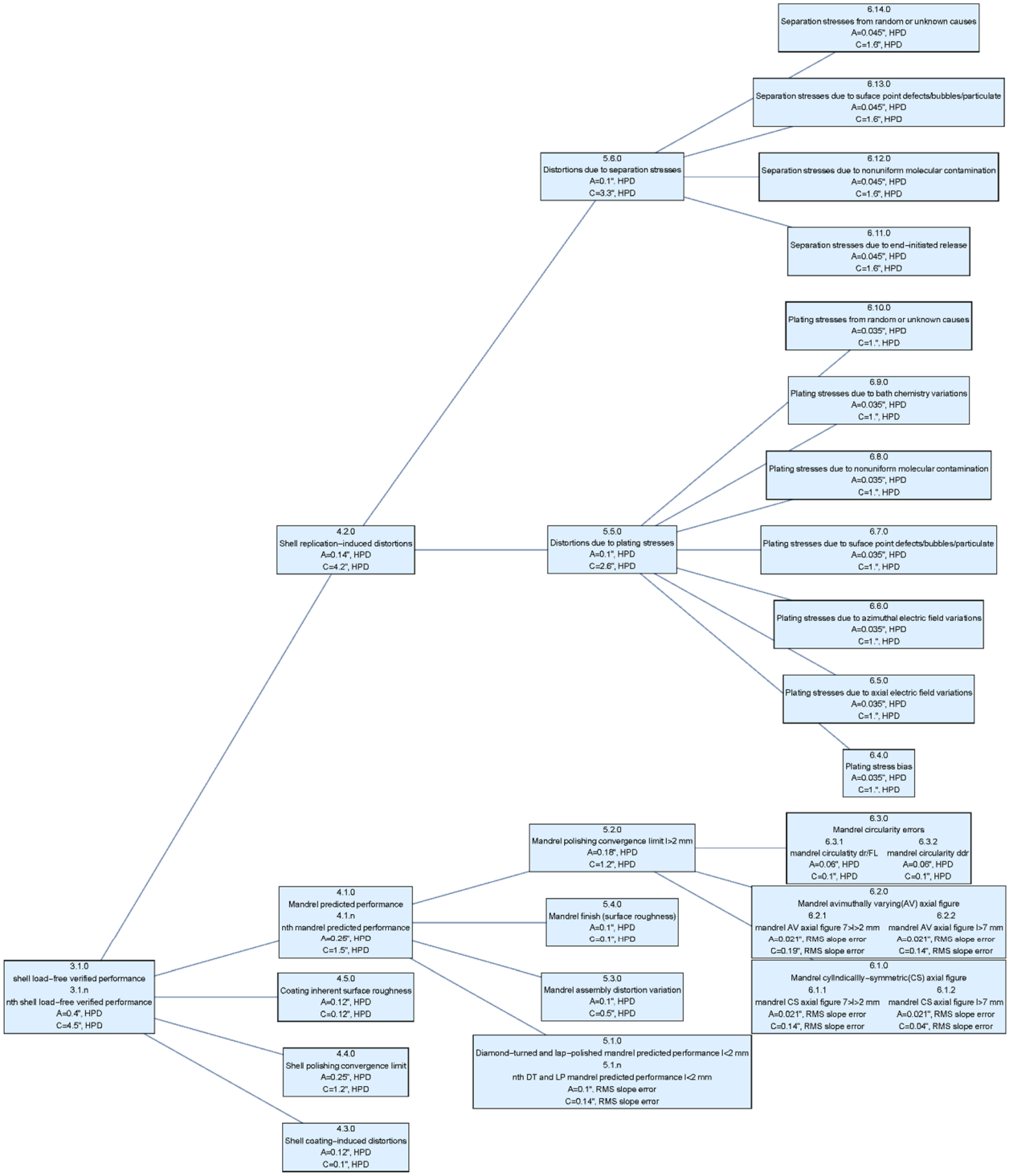

Figure 2. Error budget for shell load-free verified performance broken down to Level 6.

The error budget for shell assembly misalignment, shown in Figure 3, breaks out the error terms to Level 4. Shell performance is relatively insensitive to centering and tilt. A centering error of 1 micron and tilt error of 1 arcsec are sufficient to satisfy this allocation for a 20-m focal length, and we have already satisfied this capability when thermal compensation is applied to the assembly station [32]. For brevity we will not discuss the individual terms which were sub-allocated by equipartitioning the parent error.

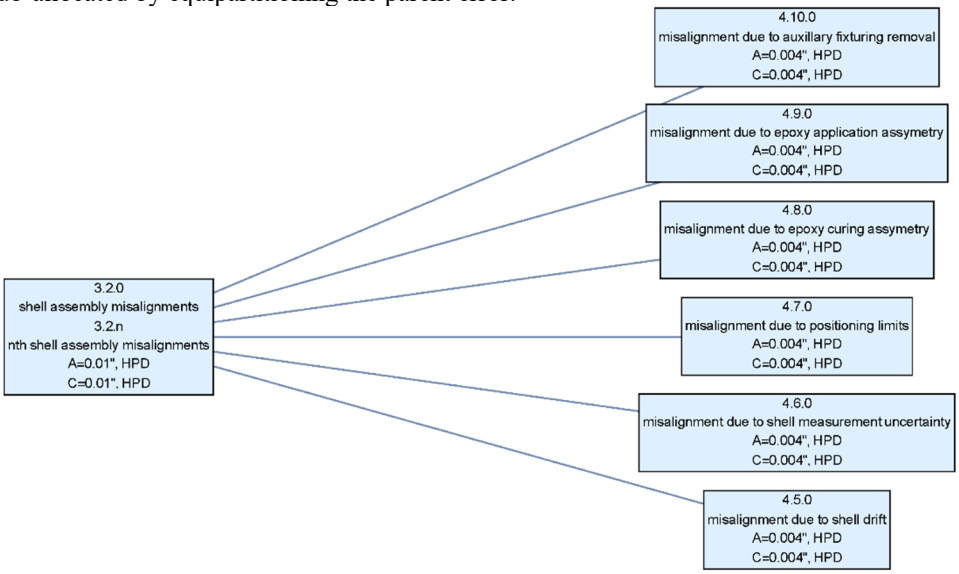

Figure 3. An error budget for shell assembly misalignments to Level 4.

Figure 4 breaks out the error terms for shell assembly distortions down to Level 4. Every step in the assembly process has a corresponding error term including suspension, stabilization, epoxy application, epoxy curing, auxiliary fixturing removal, release from the assembly station, and assembly steps after release from the assembly station. The capability is based on a best-case scenario analysis of in-situ assembly station measurements [32]. The individual Level 4 terms are sub-allocated by equipartitioning the parent errors. These values will be refined in future iterations based on analysis of in-situ data collected between assembly steps.

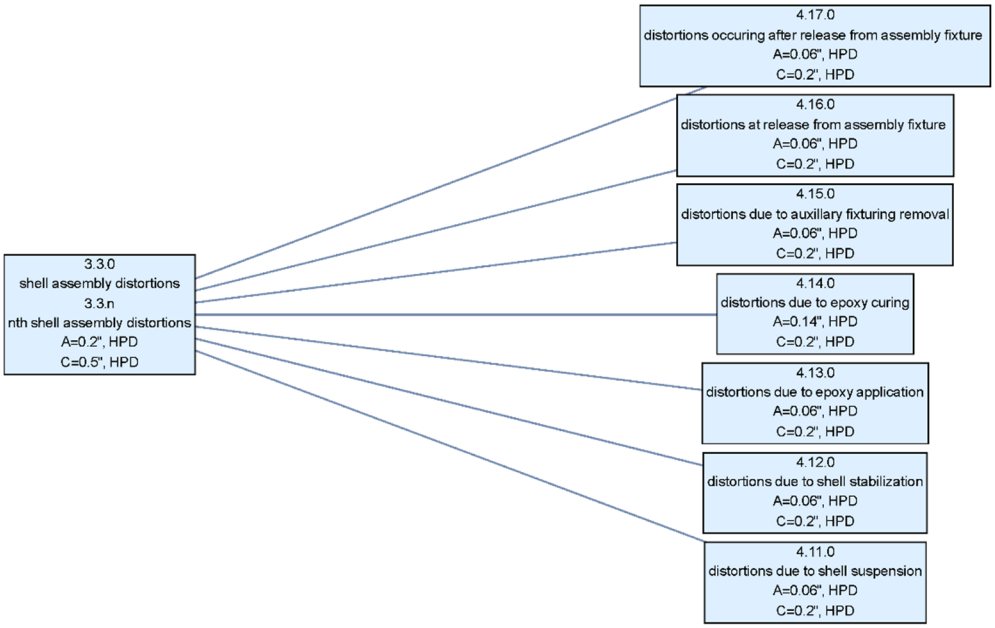

Figure 4. An error budget for shell assembly distortions to Level 4.

3.4 Generic Items

The light-orange boxes in Figure 1 are items which are not unique to replicated full shell optics. Analogous items need to be addressed for all flight-based x-ray optics technologies. Error terms contributing to ground measured x-ray performance include storage-induced changes in the shells, shell alignment with respect to the test fixture, shell distortion due to the test fixture, shell distortion due to the test environment and storage induced changes in the assembly. Using both FEM and ray-trace modeling and simulation, corrections of the ground measured performance to produce a flight prediction include, correction for shell alignment with respect to the test fixture, correction for shell distortion due to the test fixture, correction for shell distortion due to the test environment, correction for storage induced changes in the assembly, gravity-induced corrections, finite-to-infinite source corrections, thermal environment corrections, and final assembly process (post-ground test) corrections. Allocations are estimated based on *Chandra* experience and capabilities are placeholders as these items are not currently the focus of our R&D efforts.

Error terms due to potential in-flight changes include stress-induced creep in epoxies, shells or other components, long-term epoxy shrinkage and radiation-induced property changes. While such terms have had negligible effect on *Chandra*, the closely nested thin optics will be more susceptible. We do not anticipate that these items will be large contributors to the angular resolution and so at this stage carry the allocations and capabilities as placeholders.

4. PATH FORWARD

The error budget simplifies communication. Our R&D activities at MSFC boil down to advancing capabilities toward allocations. Priorities are established objectively by focusing on the areas with the highest negative margins.

Of the items directly feeding into x-ray test performance, the mirror shell performance is the tall pole, still more than a factor of 10 away from the allocation of 0.4” HPD. Among the contributors to mirror shell performance, shell replication-induced distortions dominate. This is why we have focused our efforts toward modeling the replication process. Just by optimizing gaskets and shields, in combination with shell thickness, we have gained a factor of 4-5 in HPD for relatively small shells. Continuing efforts in this area will include both the plating and separation aspect of replication. Figure 2 shows a breakdown of both these terms into potential contributors. The next step is to go from equally dividing errors among these contributors to finding ways of discriminating among them. An efficient way to distinguish between separation stress and plating stress is to vary the adhesion at the plating interface. To distinguish among the various separation stresses requires instrumenting the adhered shells in the separation bath to detect where separation begins and its subsequent propagation. Plating stress is static and already multi-physics modeled. As a result, many of these contributors are constrained through FEM, however one can ask if non-uniform plating stresses lead to specific separation scenarios which may be more or less likely to produce separation-induced distortions.

Progress requires demonstration, but end-to-end process demonstrations are costly and opportunities for these demonstrations are limited. A sufficient test needs to address replication and assembly distortions. Alignment and mandrel polishing are assumed adequate for our immediate focus. A mirror shell of at least 0.25 m in diameter is needed to examine the influence of size on the angular resolution and allows us to take the next step in capability at a more relevant scale for future astrophysics missions.

5. CONCLUSIONS

In the last 5-7 years, MSFC has significantly improved x-ray optics capabilities in mandrel fabrication, replication, and assembly. In mandrel fabrication, enhanced end-to-end polishing procedures have resulted in improving mandrel performance from 8-10” to 1.5-2.0” HPD. In replication, process simulation and monitoring feeding back into improved design has improved our replication capability from 8-10” to 4-6” HPD. Similarly, in assembly, process engineering improvements to assembly stations and assembly procedures fully achieved required alignment capabilities and improved assembly distortions from 15-20” to 0.5-1.0”. Combined overall capabilities have improved from 20-25” to 4.5-6.5”, and we are working on demonstrating this for larger-diameter shells.

High-resolution full-shell replicated optics is a feasible option for future x-ray mission. While realization depends on further progress in replication, enhancing the process with direct shell polishing remains an option if replication proves to be limited. We continue to view this technology as a healthy candidate for future large-scale astrophysics missions, and are considering related manufacturing cost factors as we progress in our R&D efforts.

While cost is not the subject of this paper, a brief calculation can give some perspective. High resolution for this technology depends fundamentally on deterministic computer-controlled polishing precision achievable on mandrel

surfaces and, if necessary, shell surfaces. This process dominates the cost model. We have attained polishing rates as high as 1.25 mm^3/hr and produced mandrels ready for CNC polishing with peak-to-peak errors below 500 nm, meaning on average 250 nm needs to be removed from a given area of the surface. Optimistically, the magnitude of the volume of material per 100 nm p-p error to be removed by CNC polishing for a *Lynx*-like system is roughly $2x10^8$ $mm^2 \times 0.00005$ mm, or 10,000 mm^3. So at minimum, the effort requires 8,000 machine-hours per 100 nm p-p error. This value suggests a competitive feasible solution is attainable.

Multiplying factors are required to get a current capability number for our process. The quoted wear-rate is based on a polishing tool for low frequencies, <0.05 mm^{-1}. To remove higher frequency requires smaller tooling which has lower wear-rates. A multiplier of roughly 3 for wear rate and 5 for initial error state gives about 120,000 machine hours. A factory with 10 CNC polishing stations operating at 70% duty cycle could complete the task within two years. The calculation doesn't include the advantage of replication that in a multiple module design, where the same mandrel can make a shell for each module. So the number of modules is a divisor in the full effort. It also points out sensitivities such as the initial state of the mandrel. A diamond-turning/lap-polishing process that produces mandrels with smaller overall p-p error and less high-spatial-frequency error could easily cut the machine hours by a factor of 2.

The above discussion on manufacturing optimization and cost indicates that the error budget alone is not sufficient to guide our development effort. Using the approach outlined in Sec 2.4, we need to understand process step effects, not just performance, but also cost, by exercising, modeling, and optimizing the end-to-end process.

ACKNOWLEDGEMENTS

The primary source of funding for this work is through the NASA Astrophysics Division Internal Scientist Funding Model (ISFM). The authors would like to recognize the MSFC Optical Systems Design & Fabrication Branch (ES23) for their efforts supporting the X-Ray Optics ISFM tasks.

REFERENCES

[1] "The *Chandra* Proposers' Observatory Guide", Version 25.0, December 2022 (Prepared by: *Chandra* X-ray Center *Chandra* Project Science, MSFC *Chandra* IPI Teams).
[2] "*XMM-Newton* Users Handbook", Issue 2.21, 17.07.2023 (ESA: XMM-Newton SOC).
[3] Bavdaz, M. et al. "NewATHENA Optics Technology," *Optics for EUV, X-Ray, and Gamma-Ray Astronomy XI*. SPIE, Paper 12679-1, 2023 (in press).
[4] "Lynx Concept Study Report", https://www.lynxobservatory.com/report
[5] Brissenden, Roger JV, and Generation-X. Team. "The Generation-X Vision Mission Study and Advanced Mission Concept." *AAS/High Energy Astrophysics Division# 10* 10 (2008): 37-03.
[6] Reid, Paul B., et al. "Constellation-X to Generation-X: evolution of large collecting area moderate resolution grazing incidence x-ray telescopes to larger area high-resolution adjustable optics." *UV and Gamma-Ray Space Telescope Systems*. Vol. 5488. SPIE, 2004.
[7] Bilbro, J. "Fabrication of a prototype mirror for AXAF-S." *Space Programs and Technologies Conference and Exhibit*. 1993.
[8] Jones, William. "Advanced X-ray mirror technology." *Space Programs and Technologies Conference*. 1996.
[9] Engelhaupt, D. E., et al. *Replicate Wolter-I x-ray mirrors*. No. NASA-TM-111117. 1994.
[10] Ramsey, Brian D., et al. "Development of hard x-ray optics at MSFC." *X-Ray and Gamma-Ray Telescopes and Instruments for Astronomy*. Vol. 4851. SPIE, 2003.
[11] Ramsey, Brian D. "Replicated nickel optics for the hard-x-ray region." *Experimental Astronomy* 20 (2005): 85-92.
[12] Christe, Steven D., et al. "The high energy replicated optics to explore the sun mission: a hard x-ray balloon-borne telescope." *Solar Physics and Space Weather Instrumentation V*. Vol. 8862. SPIE, 2013.
[13] Gubarev, M., et al. "The Marshall Space Flight Center development of mirror modules for the ART-XC instrument aboard the Spectrum-Roentgen-Gamma mission." *Space Telescopes and Instrumentation 2012: Ultraviolet to Gamma Ray*. Vol. 8443. SPIE, 2012.
[14] Gubarev, M., et al. "Development of mirror modules for the ART-XC instrument aboard the Spectrum-Roentgen-Gamma mission." *Optics for EUV, X-Ray, and Gamma-Ray Astronomy VI*. Vol. 8861. SPIE, 2013.

[15] Gubarev, M., et al. "ART-XC/SRG: status of the x-ray optics development." *Space Telescopes and Instrumentation 2014: Ultraviolet to Gamma Ray*. Vol. 9144. SPIE, 2014.
[16] Ramsey, Brian D., et al. "IXPE mirror module assemblies." *Optics for EUV, X-Ray, and Gamma-Ray Astronomy IX*. Vol. 11119. SPIE, 2020.
[17] Ramsey, B. D. "Optics for the imaging x-ray polarimetry explorer." *Optics for EUV, X-Ray, and Gamma-Ray Astronomy VIII*. Vol. 10399. SPIE, 2017.
[18] Hong, Jaesub, et al. "SmallSat solar axion and activity x-ray imager (SSAXI)." *UV, X-Ray, and Gamma-Ray Space Instrumentation for Astronomy XXI*. Vol. 11118. SPIE, 2019.
[19] Champey, Patrick, et al. "X-ray evaluation of the Marshall Grazing Incidence X-ray Spectrometer (MaGIXS) nickel-replicated mirrors." *Optics for EUV, X-Ray, and Gamma-Ray Astronomy IX*. Vol. 11119. SPIE, 2019.
[20] Champey, P. R., et al. "The Marshall Grazing Incidence X-ray Spectrometer (MaGIXS)." *Journal of Astronomical Instrumentation* 11.02 (2022): 2250010.
[21] Vogel, J. K., et al. "Design and raytrace simulations of a multilayer-coated Wolter x-ray optic for the Z machine at Sandia National Laboratories." *Review of Scientific Instruments* 89.10 (2018).
[22] Ames, Andrew, et al. "Characterization of multilayer coated replicated Wolter optics for imaging x-ray emission from pulsed power." *Optics for EUV, X-Ray, and Gamma-Ray Astronomy VIII*. Vol. 10399. SPIE, 2017.
[23] Wu, M., et al. "Characterization and calibration of a multilayer coated Wolter optic for an imager on the Z-machine at Sandia National Laboratories." *Review of Scientific Instruments* 89.10 (2018).
[24] Champey, PR., et al., "Toward the fabrication of a 5-mu m-resolution Wolter microscope for the National Ignition Facility (invited)." *Rev. Sci. Instrum.*, v. 93, 113504 (2022)
[25] O'Dell, Stephen L., et al. "X-ray optics at NASA marshall space flight center." *EUV and X-ray Optics: Synergy between Laboratory and Space IV*. Vol. 9510. SPIE, 2015.
[26] Hussey, Daniel S., et al. "Design of a neutron microscope based on Wolter mirrors." *Nuclear Instruments and Methods in Physics Research Section A: Accelerators, Spectrometers, Detectors and Associated Equipment* 987 (2021): 164813.
[27] Pivovaroff, M. J., et al. "Progress of focusing x-ray and gamma-ray optics for small animal imaging." *Penetrating Radiation Systems and Applications VII*. Vol. 5923. SPIE, 2005.
[28] Krucker, Säm, et al. "The focusing optics X-ray solar imager (FOXSI)." *Optics for EUV, X-Ray, and Gamma-Ray Astronomy V*. Vol. 8147. SPIE, 2011.
[29] Christe, Steven, et al. "Foxsi-2: Upgrades of the focusing optics x-ray solar imager for its second flight." *Journal of Astronomical Instrumentation* 5.01 (2016): 1640005.
[30] Glesener, Lindsay, et al. "The FOXSI solar sounding rocket campaigns." *Space Telescopes and Instrumentation 2016: Ultraviolet to Gamma Ray*. Vol. 9905. SPIE, 2016.
[31] Baumgartner, Wayne, et al. “High resolution full shell replicated x-ray optics for FOXSI-4.” *Optics for EUV, X-Ray, and Gamma-Ray Astronomy XI*. SPIE, Paper 12679-11, 2023 (in press).
[32] Bongiorno, Stephen D., et al. "Assembly of the FOXSI-4 Mirror Modules." *Optics for EUV, X-Ray, and Gamma-Ray Astronomy XI*. SPIE, Paper 12679-12, 2023 (in press).
[33] Marshall, Herman L., et al. “Status of the rocket experiment demonstration of a soft x-ray polarimeter (REDSoX)”, *UV, X-Ray, and Gamma-Ray Space Instrumentation for Astronomy XXIII.* SPIE, Paper 12678-40, 2023 (in press).
[34] Marshall, Herman L., et al. "The rocket experiment demonstration of a soft x-ray polarimeter (REDSoX Polarimeter)." *UV, X-Ray, and Gamma-Ray Space Instrumentation for Astronomy XX*. Vol. 10397. SPIE, 2017.
[35] Bongiorno, S. et al., “Assembly of the *IXPE* mirror modules”, *proc. SPIE*, 11822, 118220Y. doi:10.1117/12.2594316 (2021).
[36] Thomas, Nicholas E., et al. "The Marshall 100-meter x-ray beamline." *Optics for EUV, X-Ray, and Gamma-Ray Astronomy X*. Vol. 11822. SPIE, 2021.
[37] Singam, P. et al. “Optimizing the electroforming process to enhance the thickness uniformity of full shell x-ray optics”, *Optics for EUV, X-Ray, and Gamma-Ray Astronomy XI*. SPIE, Paper 12679-10, 2023 (in press).
[38] Zhang, W. et al. “Silicon x-Ray mirror technology for astronomy: high resolution, light weight, and low cost”, *Optics for EUV, X-Ray, and Gamma-Ray Astronomy XI*. SPIE, Paper 12679-14, 2023 (in press).